Quantum Chemistry: Molecular Dynamics Study of the Dark-Adaptation Process in Bacteriorhodopsin

Ilya Logunov and Klaus Schulten*

Contribution from the Beckman Institute and Departments of Chemistry and Physics, University of Illinois at Urbana−Champaign, 405 North Matthews Avenue, Urbana, Illinois 61801

Received September 7, 1995. Revised Manuscript Received July 29, 1996[⊗]

Abstract: Molecular dynamics simulations and quantum chemistry calculations have been combined to describe the dark adaptation in bacteriorhodopsin (bR). The process involves the reversible thermally activated transformation of retinal from an all-trans to a 13-*cis*,15-*syn* configuration. The potential surface governing the thermal isomerization of retinal around two (13−14, 15−N) double bonds has been determined for representative protein configurations taken from molecular dynamics trajectories. CASSCF(8,8)/6-31G level *ab initio* calculations (within Gaussian94) were carried out for this purpose. The charge distributions of all atoms in the protein are represented by partial point charges and explicitly included in the electronic Hamiltonian. Placement of retinal into bR is found to reduce the calculated isomerization barrier. Thermal fluctuations of the protein lead to a further effective reduction of this barrier. The isomerization process is shown to be catalyzed by the protonation of an aspartic acid (Asp85) side group of bacteriorhodopsin.

Introduction

Bacteriorhodopsin (bR)[1] is a protein composed of seven α-helices which spans the purple membrane of *Halobacterium halobium* and which functions as a light-driven proton pump. It is a member of the retinal protein family, which encompasses proteins with a retinal chromophore bound within the protein interior via a protonated Schiff base linkage to a lysine side chain. Figure 1a shows the chemical structure of retinal and its conventional numbering scheme. The retinal isomer composition in bR is 66% 13-*cis* and 34% all-*trans* in the dark-adapted form of the pigment (DA), a ratio which is altered in mutants of bR and in bacterial rhodopsins of other species.[1] The two isomers, denoted bR_{548} (13-*cis*) and bR_{568} (all-*trans*), absorb at 548 and 568 nm, respectively. Retinal in the bR_{568} pigment exists in an all-*trans*, 15-*anti* configuration and in the bR_{548} pigment in an 13-*cis*,15-*syn* cvonfiguration as suggested originally on the basis of semi-empirical quantum chemical calculations[2] and observed by Resonance Raman experiments.[3−5]

Both the bR_{568} and the bR_{548} isomers undergo a characteristic photocycle (see Figure 2) initialized in both cases by a photoisomerization involving rotation around the 13−14 double bond. However, proton pumping is restricted to the photocycle of bR_{568}. The photocycle of bR_{548} does not involve vectorial proton translocation.[6] The photocycle of native bR_{548} leaks into the bR_{568} form whereas the bR_{568} photocycle replenishes only the bR_{568} form. As a result, under the influence of light any mixture of bR_{568}/bR_{548} eventually becomes a pure bR_{568} pigment which, accordingly, is called the light-adapted form. The photocycles of bacteriorhodopsin are discussed in detail in recent reviews.[7−12]

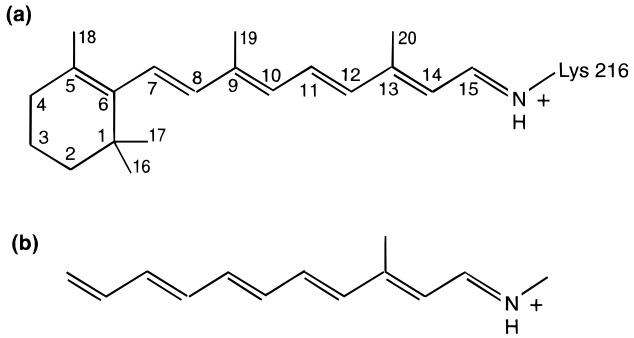

Figure 1. (a) Numbering scheme of the retinal chromophore bound via a protonated Schiff base linkage to a lysine side chain of bacteriorhodopsin; (b) retinal analogue employed in our quantum chemical calculations.

A widely accepted model for the three-dimensional structure of bR has been provided by Henderson and co-workers using electron microscopy at low temperature[13,14] together with bR's amino acid sequence.[15,16] The observations resulted in a structure for the membrane-spanning helical portion of bR at a resolution of 3 Å in a direction parallel to the membrane and at a resolution of 10 Å perpendicular to the membrane. This structure provided an opportunity to explore, by means of

* To whom correspondence should be addressed. E-mail: kschulte@ks.uiuc.edu.

[⊗] Abstract published in *Advance ACS Abstracts,* September 15, 1996.

(1) Mukohata, Y.; Ihara, K. K.; Uegaki, Y. M.; Sugiyama, Y. *J. Photochem. Photobiol.* **1991**, *54*, 1039.
(2) Orlandi, G.; Schulten, K. *Chem. Phys. Lett.* **1979**, *64*, 370.
(3) Harbison, G.; Smith, O.; Pardoen, J.; Winkel, C.; Lugtenburg, J.; Herzfeld, J.; Mathies, R.; Griffin, R. *Proc. Natl. Acad. Sci. U.S.A.* **1984**, *81*, 1706.
(4) Smith, S.; Myers, A.; Pardoen, J.; Winkel, C.; Mulder, P.; Lugtenburg, J.; Mathies, R. *Biophysics* **1984**, *81*, 2055.
(5) Livnah, N.; Sheves, M. *J. Am. Chem. Soc.* **1993**, *115*, 351.
(6) Logunov, I.; Humphrey, W.; Schulten, K.; Sheves, M. *Biophys. J.* **1995**, *68*, 1270.
(7) Khorana, H. G. *J. Biol. Chem.* **1988**, *263*, 7439.
(8) Birge, R. R. *Annu. Rev. Phys. Chem.* **1990**, *41*, 683.
(9) Mathies, R. A.; Lin, S. W.; Ames, J. B.; Pollard, W. T. *Annu. Rev. Biochem. Bioeng.* **1991**, *20*, 491.
(10) Lanyi, J. K. *J. Bioenerg. Biomembr.* **1992**, *24*, 169.
(11) Oesterhelt, D.; Tittor, J.; Bamberg, E. *J. Bioenerg. Biomembr.* **1992**, *24*, 181.
(12) Schulten, K.; Humphrey, W.; Logunov, I.; Sheves, M.; Xu, D. *Isr. J. Chem.* **1995**, *35*, 447.
(13) Henderson, R.; Unwin, P. N. T. *Nature* **1975**, *257*, 28.
(14) Henderson, R.; Baldwin, J. M.; Ceska, T. A.; Zemlin, F.; Beckmann, E.; Downing, K. H. *J. Mol. Biol.* **1990**, *213*, 899.
(15) Ovchinnikov, Y. A.; Abdulaev, N. G.; Feigina, M. Y.; Kiselev, A. V.; Lobanov, N. A. *FEBS Lett.* **1979**, *100*, 219.
(16) Khorana, H. G.; Gerber, G. E.; Herlihy, W. C.; Gray, C. P.; Anderegg, R. J. *Proc. Natl. Acad. Sci. U.S.A.* **1979**, *76*, 5046.

S0002-7863(95)03091-5 CCC: $12.00

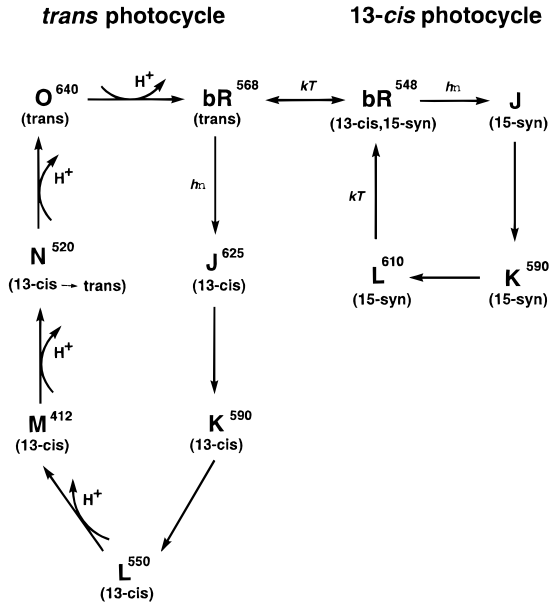

Figure 2. Photocycles of bacteriorhodopsin. Shown are the bR_{568} and bR_{548} photocycles. Superscripts on intermediates indicate measured absorption maxima of these states. Isomerization configurations of retinal in every state are indicated in brackets. Steps involving photoinduced or thermal isomerization of retinal, as well as proton transfer reactions, are marked accordingly.

computer simulations, the mechanism of bR's light-driven proton pump at the atomic level. MD simulations have been used to refine the structure of Henderson *et al.*[17] and to study structural properties of the bR_{568} pigment and its photocycle intermediates. The first MD simulation of bacteriorhodopsin demonstrated that the model of Henderson *et al.*[14] remains stable in such simulations and also investigated the *in situ* photoisomerization of retinal.[18] A second MD study placed water into bR and enforced a complete proton pump cycle proving that the mechanism of bR's pump cycle assigns a key role to bound water.[19] A third MD study attempted a systematic placement of water and a refinement of bR in an all-atom description.[17] This structure served to investigate the nature of the very early, so-called J and K, intermediates of bR's pump cycle,[20] the K and L intermediates, the M intermediate and its decay,[21] as well as the photocycle of bR_{548} demonstrating why the 13-*cis*,15-*syn* isomer does not pump protons.[6] These simulations, summarized in a recent review,[22] argue that retinal acts as a proton switch at the M stage of bR's photocycle and, thereby, explain the proton pump mechanism. Other MD simulations, combined with evaluations of p*K* values, investigated the pump mechanism of bR as well, suggesting that shuttling of Arg82 between the extracellular site and the retinal binding site is instrumental in the vectorial proton translocation.[23,24]

While molecular dynamics is a powerful tool for structural refinement, i.e., for the description of proteins at equilibrium, the realm of protein conformations far from equilibrium amenable to this technique is rather limited. In case of bacteriorhodopsin, processes like photoinduced and thermal isomerization of *in situ* retinal, as well as proton transfer processes (see Figure 2) require potential surfaces which need to be provided by quantum chemical methods. Transformations important for the function of bacteriorhodopsin, which are beyond the realm of molecular dynamics simulations based on standard force fields, involve the thermally activated isomerization of retinal around one or two of its double bonds. This includes the conversion of 13-*cis*-retinal to its all-*trans* isomeric state during the later stages of the bR proton pump cycle and includes also the process of dark-adaptation in bR. An understanding of these processes requires quantum chemical descriptions of the respective ground state potential surfaces of *in situ* retinal. Due to a lack of an atomic level protein structure, only crude potential energy surfaces were applied in studies of the isomerization of *in situ* retinal until recently.[25−27] The structure of Henderson *et al.*[14] and its refinement by means of molecular dynamics simulations[17−19,23,28] allow one now to explore the electronic properties and chemical transformations of retinal in a model-free environment.[29]

Major challenges arise for *ab initio* electronic structure calculations of *in situ* retinal. A first challenge originates from the strongly correlated nature of the conjugated π-electron system of retinal. Retinal belongs to the family of polyene dyes, which are well-known for their characteristic structure of alternating single and double π-electron bonds. Several research groups have studied the electronic structure and potential surfaces of conjugated polyene systems.[26,30−37] A distinct feature of the electronic structure of a conjugated polyene molecule is the existence of near-degenerate excited states and crossings between different potential surfaces for the twisted geometries of a polyene chain.[38−42] The most efficient way of handling near-degenerate states in quantum chemical calculations is through a multiconfigurational (MCSCF) treatment.[43−46] Electronic correlation effects can be taken into account further by performing configuration interaction (CI) calculations.[47−50] However, the use of CI calculations on top of an *ab initio* MCSCF treatment is computationally prohibitive for almost any

(17) Humphrey, W.; Logunov, I.; Schulten, K.; Sheves, M. *Biochemistry* **1994**, *33*, 3668.
(18) Nonella, M.; Windemuth, A.; Schulten, K. *J. Photochem. Photobiol.* **1991**, *54*, 937.
(19) Zhou, F.; Windemuth, A.; Schulten, K. *Biochemistry* **1993**, *32*, 2291.
(20) Xu, D.; Martin, C.; Schulten, K. *Biophys. J.* **1996**, *70*, 453.
(21) Xu, D.; Sheves, M.; Schulten, K. *Biophys. J.* **1995**, *69*, 2745.
(22) Schulten, K.; Humphrey, W.; Logunov, I.; Sheves, M.; Xu, D. *Isr. J. Chem.* **1995**, *35*, 447.
(23) Scharnagl, C.; Hettenkofer, J.; Fischer, S. F. *Int. J. Quantum Chem.* **1994**, *21*, 33.
(24) Scharnagl, C.; Hettenkofer, J.; Fisher, S. *J. Phys. Chem.* **1995**, *99*, 7787.
(25) Warshel, A. *Nature* **1976**, *260*, 679.
(26) Warshel, A. *Proc. Natl. Acad. Sci. U.S.A.* **1978**, *75*, 2558.
(27) Birge, R. R. *Biochim. Biophys. Acta* **1990**, *1016*, 293.
(28) Ferrand, M.; Zaccai, G.; Nina, M.; Smith, J.; Etchesbest, C.; Roux, B. *FEBS Lett.* **1993**, *327*, 256.
(29) Warshel, A.; Chu, Z. T.; Hwang, J.-K. *Chem. Phys.* **1991**, *158*, 303.
(30) Nakanishi, K.; Arnaboldi, M.; Baloghnair, V.; Honig, B. *J. Am. Chem. Soc.* **1980**, *102*, 7945.
(31) Hudson, B. S.; Kohler, B. E.; Schulten, K. Linear polyene electronic structure and potential surfaces. In *Excited States*; Lim, E. C., Ed.; Academic Press: New York, 1982; Vol. 6, p 1.
(32) Tavan, P.; Schulten, K. *Phys. Rev. B* **1987**, *36*, 4337.
(33) Du, P.; Davidson, R. *J. Phys. Chem.* **1990**, *94*, 7013.
(34) Graham, R.; Freed, K. *J. Chem. Phys.* **1992**, *96*, 1304.
(35) Rai, S.; Buenker, R. *Indian J. Chem.* **1992**, *31*, 215.
(36) Serrano-Andreas, L.; Merchan, M.; Nebot-Gil, I.; Nebot-Gil, I.; Roos, B. *J. Chem. Phys.* **1993**, *98*, 3151.
(37) Olivucci, M.; Bernardi, F.; Celani, P.; Ragazos, I.; Robb, M. A. *J. Am. Chem. Soc.* **1994**, *116*, 1077.
(38) Schulten, K.; Karplus, M. *Chem. Phys. Lett.* **1972**, *14*, 305.
(39) Tavan, P.; Schulten, K. *J. Chem. Phys.* **1979**, *70*, 5407.
(40) Ollivuci, M.; Ragazos, I.; Bernardi, F.; Robb, M. *J. Am. Chem. Soc.* **1993**, *115*, 3710.
(41) Ollivuci, M.; Bernardi, F.; Ottani, S.; Robb, M. A. *J. Am. Chem. Soc.* **1994**, *116*, 2034.
(42) Bonacic-Koutecky, V,.; Schoffel, K.; Michl, J. *Theor. Chim. Acta* **1987**, *72*, 459.
(43) Roos, B.; Taylor, P.; Siegbahn, P. *Chem. Phys.* **1980**, *48*, 157.
(44) Lengsfield, B. *J. Chem. Phys.* **1980**, *73*, 382.
(45) Werner, H.-J. *Adv. Chem. Phys.* **1987**, *69*, 1.
(46) Shepard, R. *Adv. Chem. Phys.* **1987**, *69*, 63.
(47) Langhoff, S.; Davidson, E. *Int. J. Quantum Chem.* **1974**, *8*, 61.
(48) Hay, P.; Shavitt, I. *J. Chem. Phys.* **1974**, *60*, 2865.
(49) Tavan, P.; Schulten, K. *J. Chem. Phys.* **1980**, *72*, 3547.
(50) Tavan, P.; Schulten, K. *J. Chem. Phys.* **1986**, *85*, 6602.

length of a conjugated polyene. An alternative and very promising approach is the implementation of multireference perturbation methods, such as CASPT2.[51,52]

Another challenge arises from the need to account for the protein environment when studying the electronic structure of retinal in bR. Protein side groups in the vicinity of the retinal Schiff base strongly affect the bR absorption spectrum as shown through mutation studies.[53] These side groups affect also drastically the rates of both thermal[54] and photoisomerization[55,56] in bR. The experiments imply that the protein environment plays a crucial role in determining the physicochemical properties of retinal *in situ*.

The problem of the proper representation of the environment in electronic structure calculations of a molecule *in situ* is complex. Initially,[57,58] a combination of *in vacuo ab initio* quantum chemical and classical solvation energy calculations were carried out. Later, various techniques were developed which permit the self-consistent *ab initio* treatment of a molecule embedded in a dielectric continuum.[59−61] At present, there exist a number of *ab initio* as well as semiempirical techniques which try to account for the realistic atomic structure and charge distribution of the environment via explicit incorporation of protein (or solution) point charges in the electronic Hamiltonian.[62−69]

The present study of the dark-adaptation process in bacteriorhodopsin combines molecular dynamics and *ab initio* quantum chemistry calculations. Dark-adaptation involves a reversible thermally activated transition between the bR_{568} and bR_{548} forms which, at room temperature, occurs with a halftime of about 1 h. Dark-adaptation is believed to proceed through the co-isomerization around the 13−14 and 15−N retinal double bonds (bicycle-pedal motion). This mechanism is supported by both molecular dynamics studies of the retinal binding site in bR,[6] semiempirical calculations of the retinal ground state potential surface *in vacuo*,[2] as well as Resonance Raman measurements.[3,4] In the present work we perform *in situ ab initio* calculations of the retinal potential surface which governs dark-adaptation of bacteriorhodopsin and estimate the overall rate of dark-adaptation. We have also recently completed a combined quantum chemistry−MD study of the spectrum of bR.[70]

Methods

Molecular dynamics (MD) and *in situ* quantum chemistry calculations were performed independently of each other. All structures were generated by the MD method which utilizes empirical force fields. Z-matrices for the retinal molecule employed in *ab initio* calculations were constructed on the basis of retinal Cartesian coordinates obtained from snapshots of MD trajectories. Coordinates of all the protein charges (which were explicitly included in the electronic Hamiltonian of retinal) were taken from the same snapshots. It should be emphasized that in MD simulations, motions of the retinal molecule itself were governed by the empirical force fields (see below) and not described by a *de novo* evaluated potential surface.

Molecular Dynamics Simulations. Molecular dynamics simulations reported here are based on the refined and equilibrated structure of bR reported in Humphrey *et al*.[17] derived from the structure reported in Henderson *et al*.[14] Following Humphrey *et al*.[17] the present description involves explicit hydrogens, includes sixteen water molecules placed and equilibrated within the protein interior and assigns standard protonation states to all side groups, except to Asp-96 and Asp-115, which are assumed to be protonated.[19,71] The water molecules are modeled using TIP3P parameters.[72] The program X-PLOR[73] with the CHARMM force field[74] was used for all simulations. bR was modeled in vacuum at a temperature of 300 K. A cut-off distance of 12 Å and a dielectric constant of $\epsilon = 1$ were used for the evaluation of Coulomb forces. All simulations used the standard X-PLOR protein topology file topallh22x.pro and parameter file parallh22x.pro.

Partial charges of retinal atoms, employed in our MD simulations, were determined with Gaussian92,[75] using a Mulliken population analysis at the MP2/6-31G level. (We favored Mulliken charges to the alternative ESP-based charges,[76−78] since the distribution of retinal charges was used not only in MD simulations, but also as a tool to study effects of fluctuating protein environment on the retinal electronic structure.) The retinal topology and parameters for the equilibrium (bR_{568}) configuration are the same as those in Humphrey *et al*.,[79] with the exception of the dihedral angle rotations for the "single" and "double" bonds, which were modified to enhance the planarity of retinal and, thus, assure better convergence of the employed CASSCF quantum chemical calculations. The increased torsional rigidity of retinal for its single bonds is justified on account of the fact that double bond rotations, i.e., around the 13−14 and 15−N bond, increase the double bond character of the single bond, rendering torsional barriers higher. This effect was originally demonstrated by semiempirical MINDO-3/MNDO calculations[2] and by our *ab initio* calculations at the CASSCF-(8,8) level. Non-additivity of the retinal torsional potentials makes a parametrization of the retinal ground state potential surface difficult and cannot be captured well by empirical force fields as employed in MD simulations.

Quantum Chemical Calculations. The quantum chemistry packages Gaussian92/94[75] were employed to study the electronic structure and potential surface of *in situ* retinal. Since a treatment of the complete retinal is computationally prohibitive, calculations have been performed on a retinal analog (Figure 1b) with the β-ionone ring and the C_9-

(51) Roos, B.; Serranoandres, L.; Merchan, M. *Pure Appl. Chem*. **1993**, *65*, 1693.
(52) Serrano-Andreas, L.; Lindh, R.; Roos, B.; Merchan, M. *J. Phys. Chem*. **1993**, *97*, 9360.
(53) Turner, G. J.; Miercke, L. J. W.; Thorgeirsson, T. E.; Kliger, D. S.; Betlach, M. C.; Stroud, R. M. *Biochemistry* **1993**, *32*, 1332.
(54) Balashov, S. P.; Govindjee, R.; Kono, M.; Imasheva, E.; Lukashev, E.; Ebrey, T. G.; Crouch, R. K.; Menick, D. R.; Feng, Y. *Biochemistry* **1993**, *32*, 10331.
(55) Kobayashi, T.; Terauchi, M.; Kouyama, T.; Yoshizawa, M.; Taiji, M. *SPIE J*. **1990**, *1403*, 407.
(56) Song, L.; El-Sayed, M. A.; Lanyi, J. K. *Science* **1993**, *261*, 891.
(57) Chandrasekhar, J.; Smith, S. F.; Jorgensen, W. L. *J. Am. Chem. Soc*. **1985**, *107*, 154.
(58) Madura, J. D.; Jorgensen, W. L. *J. Am. Chem. Soc*. **1986**, *108*, 2517.
(59) Miertus, S.; Scrocco, E.; Tomasi, J. *Chem. Phys*. **1981**, *55*, 117.
(60) Miertus, S.; Tomasi, J. *Chem. Phys*. **1982**, *65*, 239.
(61) Tannor, D.; Marten, B.; Murphy, R.; Friesner, R.; Sitkoff, D.; Nicholls, A.; Rignalda, M.; Doddard, W.; Honig, B. *J. Am. Chem. Soc*. **1994**, *116*, 11875.
(62) Clementi, E. Computational aspects for large chemical systems. In *Lecture Notes in Chemistry*; Springer: New York, 1980.
(63) Thole, B. T.; Duijnen, P. T. v. *Phys. Chem*. **1982**, *71*, 211.
(64) Singh, U. C.; Kollman, P. A. *J. Comp. Chem*. **1986**, *7*, 718.
(65) Field, M. J.; Bash, P. A.; Karplus, M. *J. Comp. Chem*. **1990**, *11*, 700.
(66) Bash, P. A.; Field, M. J.; Davenport, R. C.; Petsko, G. A.; Ringe, D.; Karplus, M. *Biochemistry* **1991**, *30*, 5826.
(67) Warshel, A. *Computer Modelling of Chemical Reactions in Enzymes and Solutions*; John Wiley and Songs, Inc.: New York, 1991.
(68) Aquist, J.; Warshel, A. *Chem. Rev*. **1993**, *93*, 2523.
(69) Gao, J.; Xia, X. *Science* **1992**, *258*, 631.
(70) Logunov, I.; Schulten, K. Beckman Institute Technical Report TB-95-24.
(71) Bashford, D.; Gerwert, K. *J. Mol. Biol*. **1992**, *224*, 473.
(72) Jorgensen, W. L.; Chandrasekhar, J.; Madura, J. D.; Impey, R. W.; Klein, M. L. *J. Chem. Phys*. **1983**, *79*, 926.
(73) Brünger, A. T. *X-PLOR*; The Howard Hughes Medical Institute and Department of Molecular Biophysics and Biochemistry, Yale University, New Haven, CT, May 1988.
(74) Brooks, B. R.; Bruccoleri, R. E.; Olafson, B. D.; States, D. J.; Swaminathan, S.; Karplus, M. *J. Comp. Chem*. **1983**, *4*, 187.
(75) Frisch, M. J.; Trucks, G. W.; Head-Gordon, M.; Gill, P. M. W.; Wong, M. W.; Foresman, J. B.; Johnson, B. G.; Schlegel, H. B.; Robb, M. A.; Replogle, E. S.; Gomperts, R.; Andres, J. L.; Raghavachari, K.; Binkley, J. S.; Gonzalez, C.; Martin, R. L.; Fox, D. J.; Defrees, D. J.; Baker, J.; Stewart, J. J. P.; Pople, J. A. *Gaussian 92, Revision A*; Gaussian Inc.: Pittsburgh, PA, 1992.
(76) Breneman, C. M.; Wiberg, K. B. *J. Comp. Chem*. **1990**, *11*, 361.
(77) Singh, U. C.; Kollman, P. A. *J. Comp. Chem*. **1984**, *5*, 129.
(78) Besler, B. H.; Merz, K. M.; Kollman, P. A. *J. Comp. Chem*. **1990**, *11*, 431.
(79) Humphrey, W.; Xu, D.; Sheves, M.; Schulten, K. *J. Phys. Chem*. **1995**, *99*, 14549.

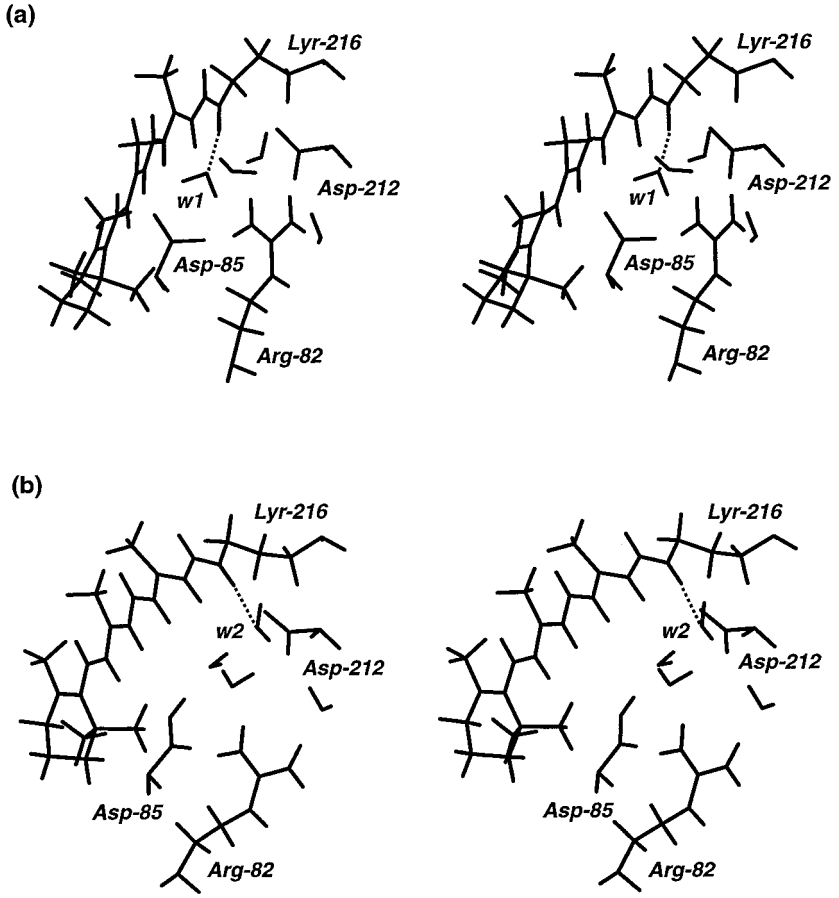

Figure 3. Stereoviews of the retinal binding site, showing retinal, water molecules, as well as key side groups: (a) structure for deprotonated Asp-85; (b) structure for the protonated state of Asp-85.

methyl groups removed. CASSCF(8,8)/6-31G level *ab initio* calculations have been carried out. Molecular orbitals obtained from the unrestricted Hartree−Fock SCF calculations have been used as an initial guess in the CASSCF calculations. The four HOMO's and four LUMO's of retinal displaying a strong π-character have been included in a complete active space (CAS) description. The convergence criterium of 10^{-4} hartree was used in all the CASSCF calculations. The protein environment was represented through explicit point charges in the electronic Hamiltonian using the CHARGE statement within Gaussian.

Computation of the Isomerization Potential Surface. *In situ* isomerization of retinal has been modeled by following a predefined reaction coordinate. Retinal was gradually rotated around the 13−14 and 15−N bonds by altering the respective dihedral angles simultaneously, i.e., bicycle peddle style, in steps of 5° and constraining these values, permitting the motions of all remaining retinal degrees of freedom to minimize the employed empirical potentials. All protein degrees of freedom were minimized according to the empirical CHARMM force field. In calculating the *in vacuo* potential surface of retinal, the same sequence of retinal conformations as in the *in situ* case had been chosen except that charges of the protein environment were not taken into account. Multiple isomerization barriers were calculated by determining the energy difference between the conformation in which retinal is co-rotated around the 13−14 and 15−N bonds by 90° and 0°, respectively. All calculations of the *in situ* potential surfaces and isomerization barriers were computed for two different protonation states of Asp-85, since it has been suggested that the protonation state of this residue controls the rate of dark-adaptation.[54]

Results and Discussion

The refined structure of bacteriorhodopsin[17] was equilibrated during 100 ps using the CHARMM22 force field and new retinal parameters depicted in Methods. Another 10 ps of molecular dynamics simulations were performed to generate protein structures utilized in the calculations of potential surfaces and the rate of dark-adaptation. We first describe briefly structural and dynamical properties of the bR binding site and then consider energetics and kinetics of the dark-adaptation process.

Atomic Structure of bR and Its Dynamical Properties. A stereoview of the retinal Schiff base region is shown in Figure 3a. The figure shows the relative position of active groups in the binding site, as well as the positions and orientations of water molecules in the region. The counterion complex of the positively charged protonated retinal Schiff base is composed of two negatively charged aspartic acids, Asp-85 and Asp-212, a positively charged Arg-82, and a few neutral water molecules. One of the water molecules (*w*1) plays the role of the primary Schiff base contact, forming a hydrogen bond with the Schiff base NH group.

Isomerization barriers of retinal are influenced by the arrangement of the surrounding side groups. All such groups, as well as retinal itself, are in thermal motion, which should play a significant role for the properties of *in situ* retinal. Shown in Figures 4a,b are time-dependent conformational properties. Figure 4a presents the motion of the 13−14 and 15−N retinal double bonds. The dihedral angles of these bonds fluctuate within a range of $180 \pm 15°$ in a strongly coherent fashion. The strong coherence of the torsions around the 13−14 and 15−N bonds shows that the protein can accommodate co-rotation around the 13−14 and 15−N retinal bonds and supports the notion that dark-adaptation occurs via a "bicycle peddle" type motion. Figure 4b shows the time dependence of the distance between the Schiff base nitrogen and the C_γ of Asp-85 and Asp-212. Both distances fluctuate within approximately 1.5 Å, which implies that Coulomb interactions between retinal and the rest of the protein are properly accounted for only after exhaustive sampling.

Time Dependence of the Isomerization Barriers. The dark-adaptation isomerization barriers have been determined for 25 snapshot structures taken every 2 ps along a 50 ps molecular dynamics trajectory. An isomerization barrier for each structure has been computed as described in the Methods section. The observed time dependence of the isomerization barriers in case of deprotonated and protonated Asp-85 is shown in Figures 5a and 5b, respectively. It is seen that the

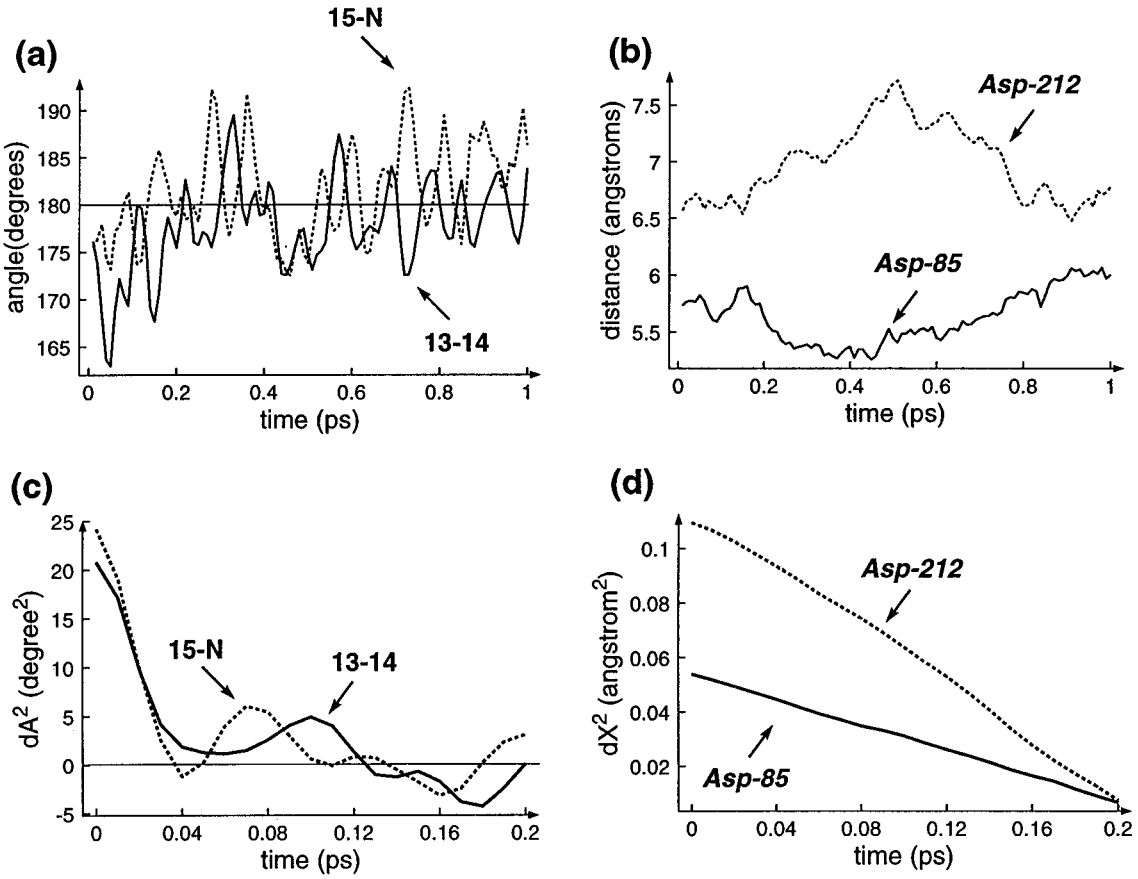

Figure 4. (a) Time dependence of the dihedral angles of the 13−14 and 15−N bonds. (b) Time dependence of the distance between the Schiff base nitrogen and the C_γ carbons of Asp-85 and Asp-212. (c) Autocorrelation function of the dihedral angles of the 13−14 and 15−N bonds. (d) Autocorrelation function of the distance between the Schiff base nitrogen and the C_γ carbons of Asp-85 and Asp-212.

barrier height values fluctuate significantly, ranging from 20 to 70 kcal/mol. The majority of points lie between 30 and 60 kcal/mol. For the deprotonated state of Asp-85, the average isomerization barrier is 51 kcal/mol, while for the protonated state the average barrier height is 43 kcal/mol. It can also be noticed that the difference between *in situ* and *in vacuo* barriers is not very significant, varying in sign and magnitude, and rarely exceeding 10 kcal/mol. Thus, one should conclude that the barrier height is controlled mainly by the internal geometry of retinal.

The internal degrees of freedom of retinal, which undergo large changes due to the thermal fluctuations and could affect considerably isomerization barriers, are the torsions around retinal's single and double bonds. The time dependence of retinal's dihedral energy is presented in Figure 6a for both protonation states of Asp-85. It is seen that dihedral energy fluctuations constitute about 6 kcal/mol which is approximately 30% of the average value of retinal's dihedral energy. It should be noticed that the average values of retinal's dihedral energy, in case of deprotonated and protonated states of Asp-85, are different, measuring respectively 19 and 16 kcal/mol. The lower average value of the dihedral energy for deprotonated Asp-85 correlates well with the lower average value of the dark-adaptation isomerization barrier. Thus, one can conclude that a higher degree of retinal twist inhibits, on average, rotation around the 13−14 and 15−N double bonds.

Potential Surface for Dark-Adaptation. We will first consider the character of the potential surface governing dark-adaptation, and later discuss how fluctuations of the isomerization barrier control the rate of the dark-adaptation process. Given in Figure 7 are two sample surfaces, one for protonated and one for deprotonated Asp-85. Respective structures of the bR binding site are shown in Figures 3a,b. These two particular structures are chosen to demonstrate possible effects of retinal torsions and of the protein environment on the nature of the dark-adaptation potential surface.

The *in vacuo* potential curve shown in Figure 7b is much flatter than the one shown in Figure 7a and displays the isomerization barrier which is 18 kcal/mol lower. This difference is due to the different conformations assumed by retinal in the binding sites containing protonated and deprotonated Asp-85. The effect can be understood in terms of the strongly correlated nature of the π-electron system of retinal: rotations around particular bonds are strongly coupled to rotations around the other bonds and, thus, to the overall conformation of retinal. Distributions of dihedral angles along retinal's backbone for the structure presented in Figure 3 are shown in Figure 6b. No specific quantitative relationships between the distribution of dihedral angles along retinal and the values of isomerization barriers can be drawn. However, the general tendency for the more twisted retinal to have larger isomerization barrier is confirmed.

The placement of retinal inside the protein in one case (Figure 7a) increases and in the other case (Figure 7b) reduces the isomerization barrier governing the thermal isomerization of retinal around two (13−14 and 15−N) double bonds, by about 10 kcal/mol with respect to the *in vacuo* calculations. The question arises whether this reduction can be explained on the basis of first-order perturbation energy invoking chromophore−protein electrostatic interactions. Figures 7c,d show the effect of Coloumb interactions at the retinal binding site on the isomerization potential surface computed exactly and in the first-order perturbation theory approximation.

We denote by ΔE_c the sum of electrostatic interactions between retinal and the apoprotein evaluated in first-order perturbation theory using the conventional MD point charge model. We denote by ΔE_q the difference between *in situ* and *in vacuo* potential surfaces evaluated quantum chemically, e.g., as shown in Figures 7c,d; ΔE_q includes the polarizing effects of the protein environment. Unlike ΔE_q, the contribution ΔE_c appears to have a negligible effect on the isomerization process. It can be concluded that the standard MD force field, wehich neglects changes of retinal's electronic structure induced by the protein environment, fails to represent the potential surface of *in situ* retinal.

The effect described by ΔE_q can be rationalized as being due to the polarization of retinal's electronic system by the counterion complex of the bR binding site. A factor which affects significantly retinal's electronic structure is hydrogen bonding to the Schiff base NH group.

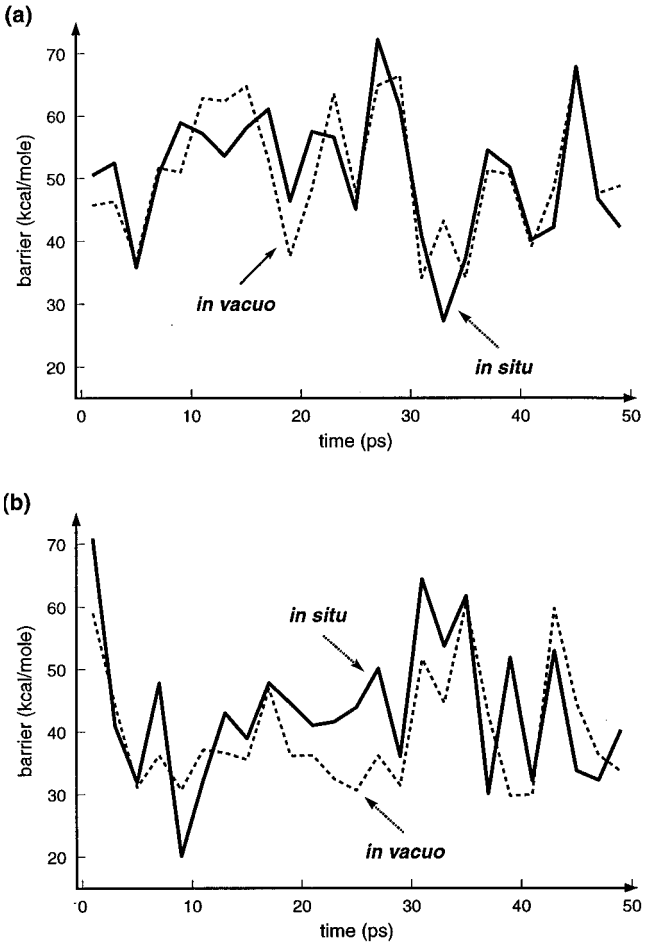

Figure 5. Time dependence of the isomerization barrier in case of deprotonated (a) and protonated (b) Asp-85. Dashed lines represent respective *in vacuo* isomerization barriers for identical retinal geometries (see text).

In our bR structure, a water molecule is engaged in such bonding (see Figure 3). A stronger hydrogen bonding to the retinal Schiff base increases electronic density in the C=N bond and should increase the isomerization barrier. This is confirmed by the two cases shown in Figures 3 and 7. In the case of deprotonated Asp-85, the strong hydrogen bonding to the Schiff base (the distance between the Schiff base hydrogen and oxygen of water *w*1 measures 1.8 Å) increases the isomerization barrier by 9 kcal/mol. In the case of protonated Asp-85, the hydrogen bonding to the Schiff base is weak (the distance between the Schiff base hydrogen and oxygen of water *w*2 measures 2.2 Å), and the isomerization barrier *in situ* is 10 kcal/mol lower than that *in vacuo*.

Rate of the Dark-Adaptation Process. We have demonstrated that the potential barrier for dark-adaptation depends on the momentary protein structure. In order to evaluate the overall rate of the dark-adaptation process, one must consider an ensemble of *trans*-bR structures and determine the distribution of energy barriers. In general, a rigorous determination of the reaction rate of a chemical process in a fluctuating environment is difficult.[80] However, simplifications can be made when the characteristic time of the environmental fluctuations is short as compared to the overall rate of the reaction, but is long as compared to the time of elementary reaction events. In this case, the effect of the environmental fluctuations can be accounted for through the static distribution of potential barriers, and integration over this distribution yields the observed reaction rate. Here we employ such a description to determine the rate of dark-adaptation of bR.

Effective Energy Barrier of Dark-Adaptation. In order to determine the rate of the dark-adaptation process for fluctuating isomerization barriers, the barriers were determined for a sample of snapshots selected from an MD trajectory. Since the protein conformational changes occur on a time scale much faster than the observed rate of dark-adaptation, the distribution $p(E)$ remains unchanged throughout the dark-adaptation process. The effective rate of dark-adaptation is then described by

$$k = k_0 \int p(E) \exp(-E/kT)\, \mathrm{d}E; \qquad \int p(E)\, \mathrm{d}E = 1 \tag{1}$$

The pre-exponential factor k_0 is a characteristic frequency for the degrees of freedom (rotations around 13−14 and 15−N bonds) which control the dark-adaptation process and can be assumed to be independent of the barrier height E. If there exists a discrete set of N barrier heights E_1, E_2, ..., E_N, eq 1 reads

$$k = k_0 \frac{1}{N} \sum_{i=1}^{N} \exp(-E_i/kT) \tag{2}$$

Matching this expression to the conventional Arrhenius expression

$$k = k_0 \exp(-E_{\mathrm{eff}}/kT) \tag{3}$$

yields

$$E_{\mathrm{eff}} = -kT \ln\left(\frac{1}{N} \sum_{i=1}^{N} \exp(-E_i/kT)\right) \tag{4}$$

Catalysis via Protonation of Asp-85. To test the hypothesis that the dark-adaptation process in bR is catalyzed by protonation of the Asp-85 side group (see Figure 8), we evaluated isomerization rates for both unprotonated and protonated states of Asp-85. Isomerization barriers were computed for 25 different structures for the two protonation states of Asp-85 (see Figure 5). We determined $E_{\mathrm{eff}} = 29$ kcal/mol for unprotonated Asp-85 and $E_{\mathrm{eff}} = 22$ kcal/mol for protonated Asp-85, i.e., protonation of Asp-85 lowers the effective barrier of dark-adaptation by 7 kcal/mol. This effect of Asp-85 protonation implies an increase of the reaction rate by four orders of magnitude. Our calculations are in a qualitative agreement with the experimental observation that transition from high pH (Asp-85 unprotonated) to low pH (Asp-85 protonated) is associated with a 1000-fold increase in the rate of dark-adaptation.[54]

Absolute Rate of Dark-Adaptation. In order to determine the absolute rate of dark-adaptation, one must obtain an estimate for the pre-exponential factor k_0. We define the characteristic frequency k_0 as the inverse of the decay time t_0 of the autocorrelation function for the torsional motions around the 13−14 and 15−N double bonds of retinal. The autocorrelation function is depicted in Figure 4c. From Figure 4c follows $t_0 \approx 2 \times 10^{-14}$ s. Thus, we obtain $k_0 \approx 5 \times 10^{13}$ s^{-1}. According to eq 3 and using $E_{\mathrm{eff}} \approx 22$ kcal/mol (see above), the rate of dark-adaptation, in the case of protonated Asp-85, is then $k_{\mathrm{prot}} = 6 \times 10^{-3}$ s^{-1} $\sim 10^{-2}$ s^{-1}. Comparison with the observed maximum rate $k_{max} = 4 \times 10^{-2}$ s^{-1} of bR dark-adaptation at low pH values, i.e., for protonated Asp-85,[54] shows that our calculations give the right order of magnitude for the absolute rate.

In evaluating the rate constant for the dark-adaptation process, a static distribution of the activation barriers was assumed. This assumption is equivalent to the postulate that the elementary act of retinal isomerization occurs on a time scale which is fast compared to the structural rearrangements within the bR binding site. To test this assumption, the characteristic time scale for the torsional motions of retinal along the reaction coordinate and the time scale for the motions of side groups in the retinal binding site were compared. For this purpose we computed the autocorrelation functions for the torsions around retinal's 13−14 and 15−N double bonds and compared them with the autocorrelation functions for the distances between the Schiff base nitrogen and C_γ carbons of Asp-85 and Asp-212, two key amino acids in the retinal binding pocket. Figure 4c,d shows that the autocorrelation function for the retinal dihedral torsions decays five times faster than the autocorrelation function of the distance between the Schiff base and aspartic acids. The observation, that fluctuations along the reaction coordinate (rotation around retinal's 13−14 and 15−N bonds) occur on a shorter time scale compared to the fluctuations

(80) Kampen, N. G. v. *Stochastic Processes in Physics and Chemistry*; North-Holland: Amsterdam, New York, 1992.

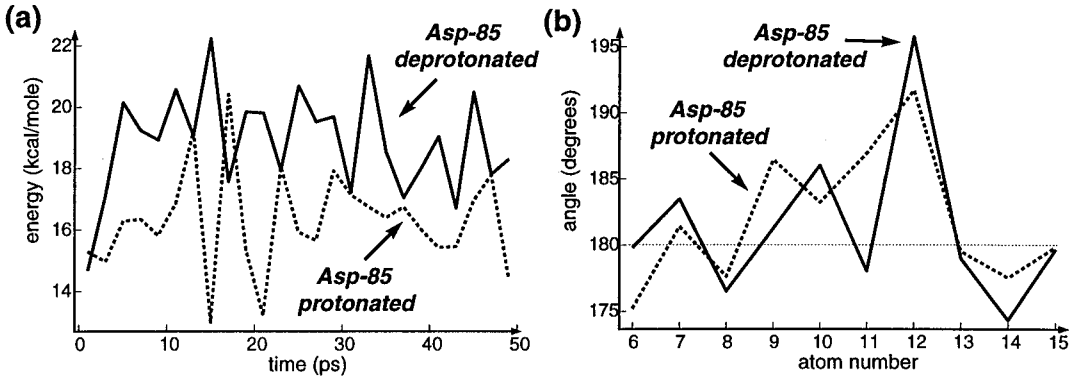

Figure 6. (a) Time dependence of the retinal dihedral energy in case of deprotonated (full line) and protonated (dashed line) Asp-85. (b) Distribution of dihedral angles along retinal's backbone in case of deprotonated (full line) and protonated (dashed line) Asp-85. The respective structures of the bR active site are shown in Figures 3a,b.

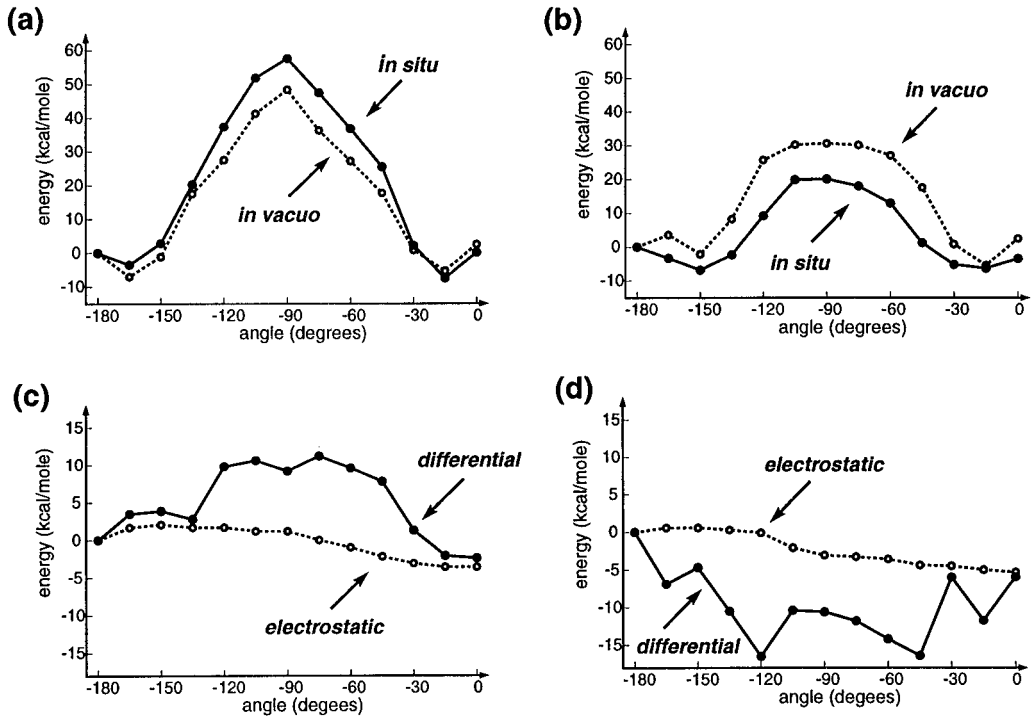

Figure 7. (a, b) Retinal ground state potential surfaces describing the dark-adaptation process in the case of deprotonated (a) and protonated (b) Asp-85. Shown are *in situ* and *in vacuo* potential surfaces obtained from the same sequence of retinal conformations. (c, d) Effect of Coulomb interactions on the dark-adaptation potential surfaces in the case of deprotonated (c) and protonated (d) Asp-85: dashed lines represent interaction energies evaluated according to first-order perturbation theory accounting for the Coulomb interaction between retinal and the protein matrix (see text); full lines represent interaction energies evaluated as the difference between the *in situ* and *in vacuo* potential curves shown in parts a, b.

of the side group positions within the bR binding site, lends support to the procedure employed for evaluating E_{eff}. However, a rigorous prove of eq 4 requires analysis of the autocorrelation function for the isomerization barrier $E(t)$ itself. Such a procedure is currently computationally prohibitive.

Elementary Act of Dark-Adaptation. The characteristic time of the elementary microscopic act of dark-adaptation can also be monitored. Activation of the torsional degrees of freedom from their equilibrium values to the twisted conformations in a transition state (see Figure 8) is a microscopic time reversal of the relaxation from the transition state to the equilibrium. Thus, simulation of such a relaxation process provides information about the elementary isomerization act.[81,82] Figure 9 portrays the behavior of the 13−14 and 15−N dihedral angles in the course of their relaxation from the transition state to equilibrium. It is seen that complete energy dissipation from the 13−14 and 15−N torsional degrees of freedom to other protein degrees of freedom occurs within a picosecond. However, the major change of the dihedral angle values occurs within 50 fs. This implies that, although energy accumulation in the reaction coordinate takes about 1 ps, the sharp jump along the reaction coordinate happens within 50 fs. This time is to be compared with the characteristic time of 200 fs for the noticeable rearrangement of protein side groups within the retinal binding site (Figure 4d). One can conclude that the assumption concerning time scale separation between the elementary isomerization act and environmental fluctuations within the retinal binding site is justified.

Accuracy of Performed Calculations. The accuracy of the performed calculations is determined by the level of *ab initio* calculations employed, by the way in which the protein environment is accounted for, by the procedure chosen to calculate the isomerization barriers of dark-adaptation, as well as by the limited statistics employed for evaluation of the overall rate of dark-adaptation. The CASSCF-(8,8)/6-31G level of *ab initio* calculations has been employed in the present work. Our sample calculations with a double-polarized basis set (6-31G**), performed on a smaller retinal analog, have demonstrated that rotation barriers around the double bonds of protonated Schiff bases essentially do not change when one uses basis sets larger than 6-31G at the CASSCF(8,8) level. Improvements in the basis set combined

(81) McCammon, J. A.; Harvey, S. C. *Dynamics of Proteins and Nucleic Acids*; Cambridge University Press: Cambridge, 1987.

(82) Brooks, C. L., III; Karplus, M.; Pettitt, B. M. *Proteins: A Theoretical Perspective of Dynamics, Structure and Thermodynamics*; John Wiley & Sons: New York, 1988.

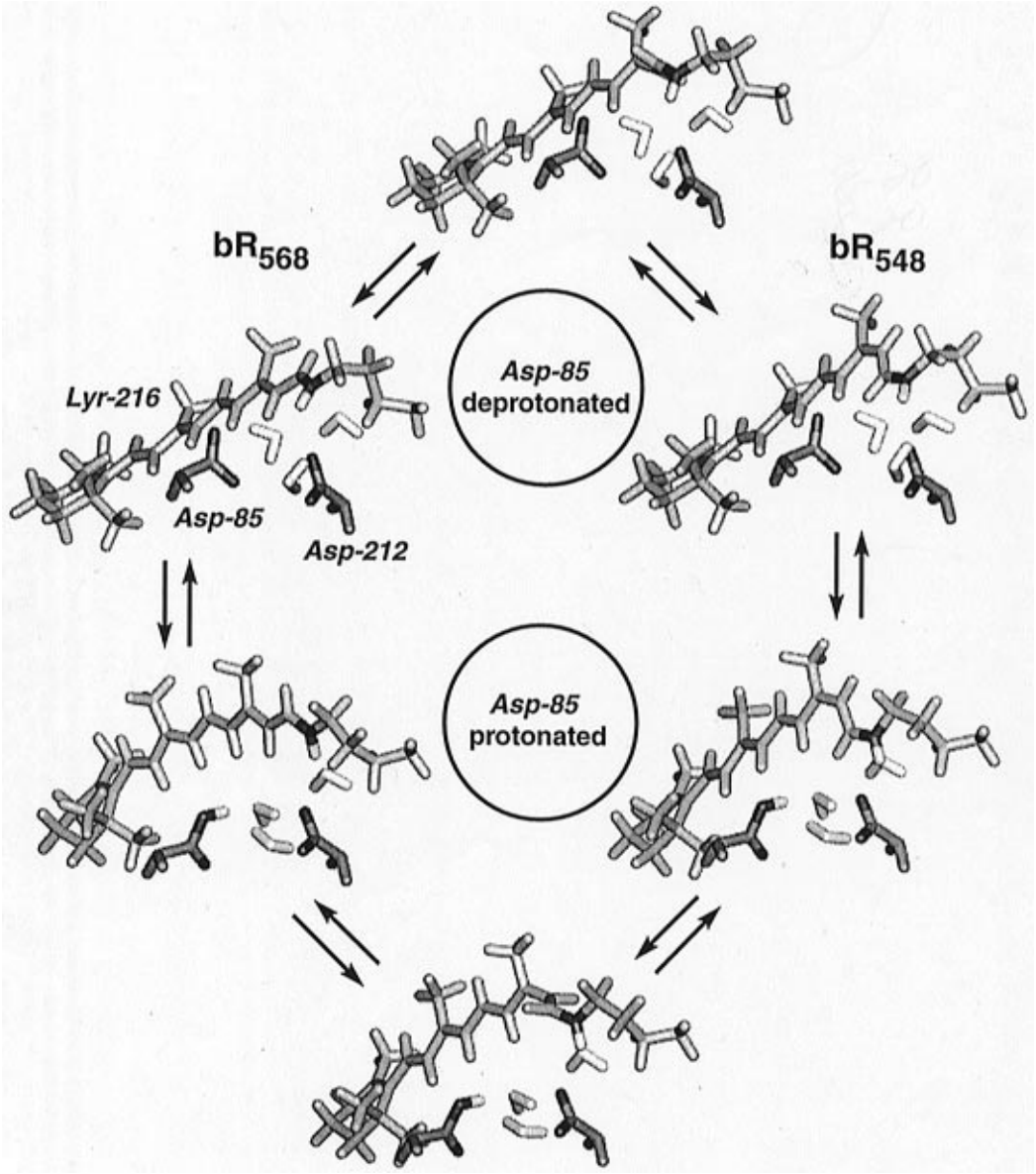

Figure 8. Sequence of retinal conformations involved in the dark-adaptation process of bacteriorhodopsin. Shown are two possible pathways. It is currently believed that dark-adaptation occurs via protonation of Asp-85 (bottom pathway).

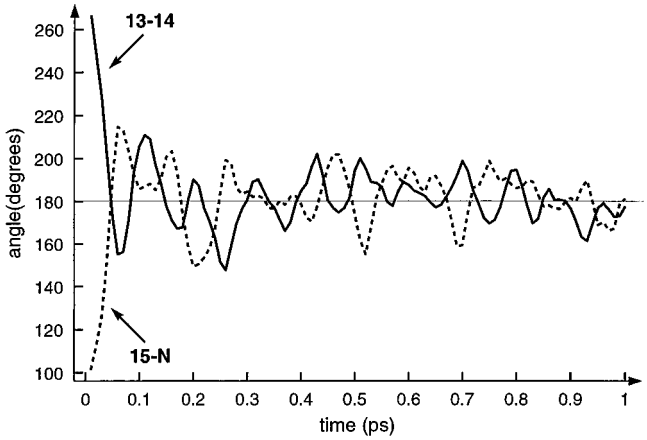

Figure 9. Time dependence of the torsional angles of the 13−14 and 15−N bonds of *in situ* retinal starting ($t = 0$) at the transition state of dark-adaptation (i.e., for an initial twist of the 13−14 and 15−N double bonds of 90°, see Figure 8); the time reversal of this process corresponds to an elementary dark adaptation event; Asp85 protonated.

with improvements in the *ab initio* level (via increase of the complete active space and implemention of configuration interaction or perturbation theory on top of CASSCF) could further improve the barriers for dark-adaptation, but such calculations are computationally prohibitive at present.

The role of the environment was taken into account by explicitly including all protein partial charges in the Hamiltonian. Improvements of the representation of the environment should account for the protein polarizability, as well as for protein atoms in direct van der Waals contact with retinal.

The co-rotation around retinal's 13−14 and 15−N double bonds has been chosen as the isomerization reaction pathway. This choice of the reaction coordinate is well justified. On the one hand, this "bicycle peddle" motion is favored by the protein environment, since it invokes the smallest possible perturbation of the surrounding groups. The *in vacuo ab initio* calculations also favor co-rotation over the sequential isomerization, e.g. all-*trans* → 13-*cis* → 13-*cis*,-15-*syn*. Calculations performed for the planar optimized retinal geometry yield isomerization barriers of 34 kcal/mol for the rotation around the 13−14 bond, 47 kcal/mol for rotation around the 15−N bond, and 47 kcal/mol for the co-rotation around the 13−14 and 15−N bonds.

The main shortcoming of the described calculations is that retinal geometries are computed by empirical potentials, while energies are determined by *ab initio* calculations. While complete *ab initio* minimization of *in situ* retinal would be more preferable, it is

computationally prohibitive. The *in situ ab initio* calculations performed in the study are already computationally very expensive. The evaluation of an isomerization barrier height for a given structure requires approximately 1 day on an HP-735/125. Thus, we had to restrict ourselves to a very limited number of data points.

Conclusions

Experimental determination and theoretical refinement of the bacteriorhodopsin structure have led to a point where detailed simulations of elementary processes occurring in the retinal binding pocket have become feasible. In the present work we have examined the dark-adapation process in bacteriorhodopsin which involves the thermally activated isomerization around two (13−14 and 15−N) retinal double bonds. *Ab initio in situ* quantum chemical calculations were performed on an ensemble of protein structures. The calculations provide important insight into the regulation of *in situ* transformtions of retinal by the protein environment. The employed level of *ab initio* calculations (CASSCF(8,8)) proved to be adequate for describing the ground state protential surface of *in situ* retinal. The calculated absolute rates of the dark-adaptation process are in accord with observations.

Our study supports the notion that steric and Coulomb interactions are the two major factors that govern chemical transformations in a protein active site.[66−68,83,84] However, our simulations also demonstrate that the effect of steric interactions is not restricted to a mere "key-lock" relationship and that Coulomb interactions cannot be properly described within first-order perturbation theory accounting for the retinal−protein electrostatic interactions. We observe that steric interactions between retinal and the protein cause conformational changes of the chromophore resulting in a noticeable change of its electronic structure and isomerization potential surface. Explicit incorporation of protein charges in the electronic Hamiltonian of retinal is of crucial importance, since the protein charge environment polarizes the chromophore and alters substantially its electronic structure.

Acknowledgment. The authors express their gratitude to Chuck Martin for helpful discussions and to William Humphrey for assistance in the preparation of the manuscript. The research was carried out at the Resource for Concurrent Biological Computing at the University of Illinois, funded by the National Institutes of Health (grant P41RR05969). The research has been supported also by the Roy J. Carver Charitable Trust. The majority of simulations were carried out on Hewlett-Packard and Silicon Graphics workstations operated by the Resource. I. Logunov received a graduate fellowship from the University of Illinois.

JA953091M

(83) Warshel, A.; Aqvist, J. *Annu. Rev. Biophys. Biophys. Chem.* **1991**, *20*, 267.

(84) Warshel, A. *Curr., Opinion Struct. Biol.* **1992**, *2*, 230.